

# Atomic Fock State Preparation Using Rydberg Blockade

Matthew Ebert,\* Alexander Gill, Michael Gibbons, Xianli Zhang, Mark Saffman, and Thad G. Walker  
 Department of Physics, University of Wisconsin,  
 1150 University Avenue, Madison, Wisconsin 53706, USA  
 (Dated: February 12, 2018)

We use coherent excitation of 3-16 atom ensembles to demonstrate collective Rabi flopping mediated by Rydberg blockade. Using calibrated atom number measurements, we quantitatively confirm the expected  $\sqrt{N}$  Rabi frequency enhancement to within 4%. The resulting atom number distributions are consistent with essentially perfect blockade. We then use collective Rabi  $\pi$  pulses to produce  $\mathcal{N} = 1, 2$  atom number Fock states with fidelities of 62% and 48% respectively. The  $\mathcal{N} = 2$  Fock state shows the collective Rabi frequency enhancement without corruption from atom number fluctuations.

Ensembles of cold neutral atoms localized in micron-sized clouds interact collectively with laser light tuned to excite  $n \sim 100$  Rydberg states. Within such clouds the interactions between two or more Rydberg atoms are many orders of magnitude greater than the interactions between ground-state atoms. Thus while a single photonic absorption is resonant, subsequent photonic absorptions are made off-resonant by Rydberg-Rydberg interactions. For sufficiently cold atoms, this "blockade" energetically constrains the  $N$  atom ensemble to an effective 2-level Hilbert space consisting of either  $N$  ground-state atoms or  $N - 1$  ground state atoms and 1 Rydberg excitation. The sharing of the excitation between the  $N$  atoms causes atom-light couplings to be collectively enhanced by  $\sqrt{N}$  [1, 2].

For  $N = 2$ , Rydberg blockade [3, 4] has been exploited to produce entanglement [5–7] and to observe  $\sqrt{2}$  Rabi enhancement [4]. Collective Rabi oscillations at large  $N$  were also recently observed [8]. When the cloud size allows multiple Rydberg excitations, blockade results in excitation suppression and dramatically increased optical non-linearities. This works even at the single photon level, [9–12] and allows entanglement of light and atomic excitations [13].

The classic signature of coherent collective behavior is collective Rabi flopping, as emphasized in the original Lukin *et al.* proposal [1]. Fluctuations in atom loading statistics produce, through the  $\sqrt{N}$  dependence, inhomogeneous broadening that dephases the collective Rabi manipulations. This is important, for example, for potential use in collective quantum gates [14], protocols for deterministic single photon sources [15], or entanglement of single-atom and collective qubits [16]. To minimize this effect, one would like to be able to reduce the atom number fluctuations below the classical Poissonian limit, also proportional to  $\sqrt{N}$ .

In this Letter we experimentally realize a collective protocol [15] for deterministic production of single and two-atom Fock states. We load an ensemble of  $3 < \bar{N} < 16$  atoms into a single dipole trap and extract single atoms via collective Rabi  $\pi$ -pulses between one ground-state hyperfine level and a Rydberg state, followed by

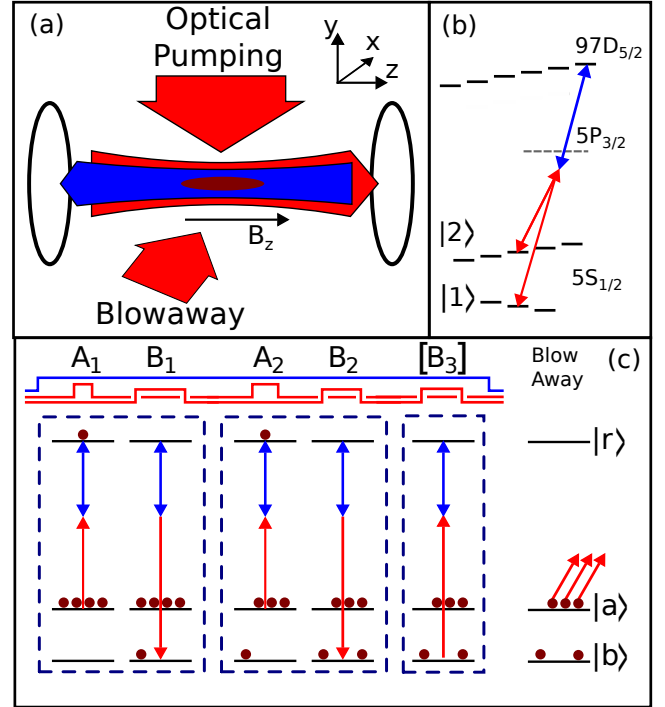


FIG. 1. (Color online) (a) Experimental geometry. Counter-propagating 780 and 480 nm Rydberg excitation lasers, parallel to an applied magnetic field, couple  $|a\rangle$  or  $|b\rangle$  to  $|r\rangle$ . Optical pumping and state selective blow away beams are incident on the ensemble in the perpendicular plane. (b) Two-photon excitation diagram. (c) Fock state generation pulse sequences. Sequential pairs of A and B excitation pulses perform population transfer from  $|a\rangle \rightarrow |r\rangle \rightarrow |b\rangle$ . Ideally, the Rydberg blockade mechanism moves a single atom to  $|b\rangle$  per A – B pulse pair. After two A – B pulse pairs, the  $B_3$  pulse optionally probes 2-atom Fock state dynamics.

stimulated emission into a second ground hyperfine level, Fig. 1(c). We quantitatively verify the  $\sqrt{N}$  enhancement factor with a precision of 4%. Subsequent sequences of such pulse pairs allows production of multi-atom Fock states. We demonstrate sub-Poissonian production of single and two-atom Fock states using this method.

Our basic apparatus is quite similar to our previous

work [6, 7]. Indeed, the collective Rabi flopping protocols are similar to protocols for single-atom qubit control, and hence are convenient for loading arrays for neutral atom quantum computing. We transfer a small number of Rb atoms (up to 30) from a magneto-optical trap into a 1.5 mK deep  $1.06 \mu\text{m}$  far-off resonance trap (FORT) focussed to a waist of  $3.0 \mu\text{m}$ . The atoms are then laser-cooled to 100-150  $\mu\text{K}$ , during which time light-assisted collisions induced by the cooling light cause atoms to be ejected from the FORT. Varying the cooling time allows us to realize a mean atom number,  $\bar{N}$ , from 0.5 to 16 atoms. Measurement of  $\bar{N}$  will be discussed later. The spatial distribution of the trapped atoms is a  $7 \mu\text{m}$  long and  $< 0.5 \mu\text{m}$  wide Gaussian distribution oriented along the FORT propagation direction. Calculations indicate that the Rydberg-Rydberg interaction [17] is 11 MHz at a typical  $12 \mu\text{m}$  atom-atom distance, sufficient for the 1 MHz scale Rabi flopping studied here. Once trapped, the atoms are optically pumped into the  $|5S_{1/2}, F=2, m_F=0\rangle$  clock state, and the FORT is turned off for 3-6  $\mu\text{s}$  while the Fock state pulse sequence is applied.

The Fock-state pulse geometry is shown in Fig. 1(a). We perform independent coherent two-photon excitations between either of the two ground states  $(|a\rangle, |b\rangle) = |5S_{1/2}, F=(2,1), m_F=0\rangle$  and the  $|r\rangle = |97D_{5/2}, m_J=5/2\rangle$  Rydberg state. Two independently switchable 780 nm lasers, with waists of  $\omega_{(x,y)} = (9,7) \mu\text{m}$ , energetically select the hyperfine level coupled to  $|r\rangle$ . Both of these lasers co-propagate with the FORT laser. A counter-propagating 480 nm beam with waists of  $\omega_{(x,y)} = (5.6, 4.7) \mu\text{m}$ , which is left on continuously, provides the second step to the Rydberg state. Each excitation laser is locked to a different mode of a high finesse cavity. The single-photon Rabi frequencies for the 2-photon transition are typically  $(\Omega_{480}, \Omega_{780}) = 2\pi \times (17, 160)$  MHz, with a -2.1 GHz detuning from the  $5P_{3/2}$  level, giving a single-atom two-photon Rabi frequency of  $\Omega_1 = 2\pi \times 750$  kHz. The timing of each pulse is controlled by the duration of the respective 780 nm beams. In the following, we refer to a Rabi oscillation between  $(|a\rangle, |b\rangle)$  and  $|r\rangle$  as an  $(A_p, B_p)$  pulse, where  $p$  refers to the pulse sequence number in Figure 1(c). All pulse times  $t$  are chosen to have pulse area  $\theta = \pi = \sqrt{N}\Omega t$ , unless explicitly noted.

Following the Fock state pulses, the number ( $N_b = 0, 1$ , or 2) of atoms in state  $|b\rangle$  is determined by first ejecting atoms from  $|a\rangle$  using resonant light [6], then collecting light from the remaining atoms while laser cooling for 20 ms. Measurements show that atoms in  $|a\rangle$  can be ejected with a fidelity of 97%. Atoms remaining in Rydberg states at the end of a pulse sequence leave the trap after the FORT is turned back on [3], so population in Rydberg states is not directly detected in this experiment.

Beginning with an  $\bar{N}$  atom ensemble initialized in  $|a\rangle$ , the  $A_1(\theta)$  pulse produces a collective Rabi oscillation between the state  $|g\rangle = |a_1 a_2 \dots a_N\rangle$  and the symmetric

singly-excited W state  $|r\rangle = N^{-1/2} \sum_{i=1}^N |a_1 a_2 \dots r_i \dots a_N\rangle$ . The  $B_1$  pulse, calibrated using single-atom Rabi oscillations out of state  $|b\rangle$ , then drives a single-atom  $\pi$  pulse between the single Rydberg atom and the unpopulated  $|b\rangle$  state. Ideally, this sequence should produce a single-atom Fock state in  $|b\rangle$ .

Figure 2 shows the results of measurements of  $N_b$  after  $A_1(\theta)B_1$  sequences. As the number of atoms is successively increased from 1 (top) to 15.5 (bottom), the Rabi frequency increases as expected from collective enhancement. We fit each data set to the following model for the probability  $p_1(t)$  for one atom to be in  $|b\rangle$  as a function of  $A_1(\theta)$  pulse time:

$$p_1(t) = \frac{\epsilon}{2} \sum_{N=0}^{N_{max}} P_{\bar{N}}(N) \left[ 1 - \cos(\sqrt{N}\Omega_1 t) e^{-t/\tau} \right], \quad (1)$$

where  $P_{\bar{N}}(N)$  is the Poisson distribution of initial atom

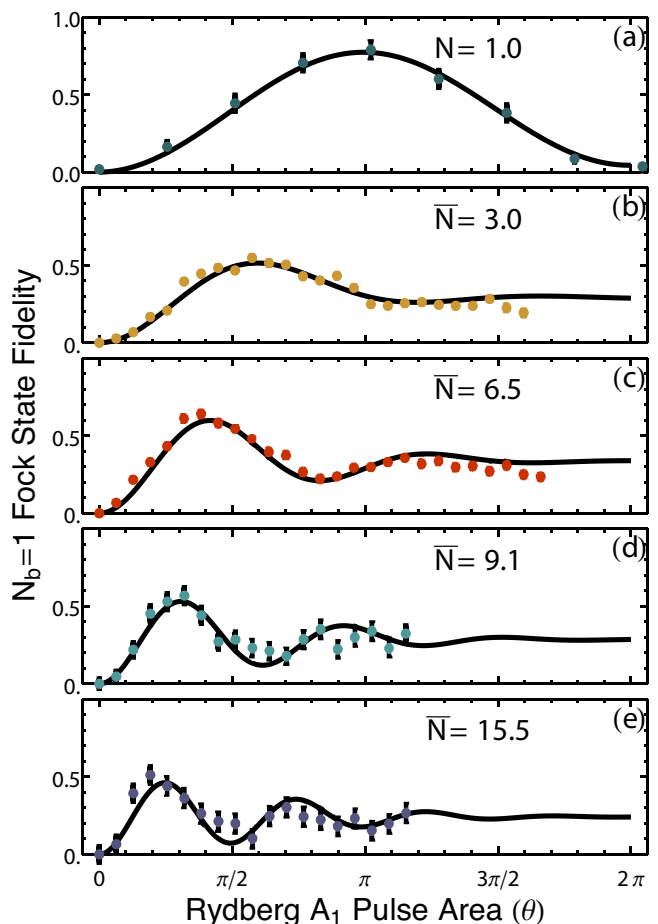


FIG. 2. (Color online) Rabi oscillations between  $|a\rangle$  and  $|r\rangle$  for various atom number distributions. The single atom detection probability is shown as a function of the pulse area  $\theta = \Omega_1 t$  of the Rydberg A excitation. (a) The first  $2\pi$  rotation for exactly one atom. (b-e) The  $|b\rangle$  populations show an atom number dependent frequency for ensemble means of, respectively,  $\bar{n} = 3.0, 6.5, 9.1, 15.5$ . The solid black lines are the fits to Eq. (1).

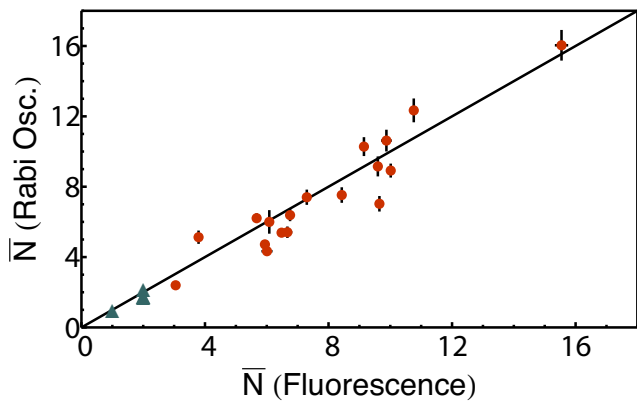


FIG. 3. (Color online) Mean number of atoms in the ensemble, as deduced from collective Rabi oscillations (ordinate), and by fluorescence (abscissa). The red circles are data from Poisson-distributed atom ensembles, the green triangles have exactly 1 or 2 atoms. The solid black line, of slope 1, shows that the collective oscillation frequency closely follows the predicted  $\sqrt{N}$  dependence.

numbers, and  $\tau$  is the decay time of the Rabi oscillations. Both  $\Omega_1$  and  $\tau$  (typically  $2\pi \times 750$  kHz and  $5 \mu\text{s}$ ) are measured from single-atom Rabi flopping. A two parameter fit for each data set returns the mean atom number  $\bar{N}$  and an overall scaling factor  $\epsilon$ , to be discussed with Fig 5.

We separately measure  $\bar{N}$  by collecting fluorescence scattered by the atoms from short (3 ms) pulses of cooling light. In the  $> 10^{11} \text{ cm}^{-3}$  density cloud, the calibration of number of scattered photons per atom is affected by significant light-assisted collision loss. In separate experiments we measure the relevant two-body loss rates and implement the relevant calibrations [18].

A comparison between  $\bar{N}$  as deduced from the collective Rabi oscillations, and from the direct atom number measurements, is shown in Fig. 3, along with a line of slope 1. The close agreement quantitatively confirms the phenomenon of collective Rabi frequency enhancement in the strong blockade limit. Allowing the slope to vary gives a best fit of 0.96.

Fig. 2 demonstrates that when the Rydberg  $A_1$  pulse area is chosen to be a collective  $\pi$ -pulse, i.e.  $\Omega_{\bar{N}}t = \pi$ , and the Rydberg  $B_1$  pulse is set to a single atom  $\pi$ -pulse, our procedure is capable of creating an  $\mathcal{N} = 1$  Fock state in which a single atom of the ensemble has been transferred to the state  $|b\rangle$  with an efficiency as high as 63.3%. The observed distribution of  $N_b$  is 35%  $N_b = 0$ , 63.3%  $N_b = 1$ , and 1.3%  $N_b = 2$ . The number of  $N_b = 2$  cases observed is consistent with our known efficiency for ejecting the atoms in  $|a\rangle$ , implying that any double Rydberg excitations due to imperfect blockade do not transfer to  $|b\rangle$ . The resulting Fock state distribution is very sub-Poissonian with a Mandel parameter  $Q = \sigma_{N_b}^2 / \bar{N}_b - 1 = -0.62 \pm 0.03$ .

The  $\mathcal{N} = 1$  Fock state preparation procedure can be

generalized to  $\mathcal{N} > 1$  by simply repeating the Rydberg  $A$  and  $B$  pulse sequence  $\mathcal{N}$  times, with each pulse area set to be a collective  $\pi$ -pulse for the number of coupled atoms. Thus the ideal collective Rabi frequencies for pulses  $A_2$  and  $B_2$  are  $\sqrt{\mathcal{N} - 1}\Omega_1$  and  $\sqrt{2}\Omega_1$ . To study  $\mathcal{N} = 2$  Fock state preparation, we first consider the possible outcomes of an  $A_1B_1$  pulse sequence followed by an  $A_2$  pulse. There are four cases  $|N_r, N_b\rangle$ :

1. neither pulse sequence succeeds:  $|0, 0\rangle$
2.  $A_1B_1$  succeeds, but  $A_2$  fails, resulting in one atom in  $|b\rangle$ :  $|0, 1\rangle$
3.  $A_1$  fails, and  $A_2$  succeeds, resulting in one Rydberg atom:  $|1, 0\rangle$
4. All pulses succeed, resulting in one atom in both  $|b\rangle$  and  $|r\rangle$ :  $|1, 1\rangle$

Finally, a fourth pulse,  $B_2(\theta)$ , couples  $|b\rangle \leftrightarrow |r\rangle$  and evokes different behavior for each possible state mentioned. For  $|0, 0\rangle$ ,  $B_2$  has no effect. Both single-atom outcomes oscillate between  $|0, 1\rangle \leftrightarrow |1, 0\rangle$  at the single atom Rabi frequency but are out of phase with each other. The  $|1, 1\rangle$  state, however, uniquely oscillates between  $|1, 1\rangle \leftrightarrow |0, 2\rangle$  at a  $\sqrt{2}\Omega_1$  enhanced Rabi frequency. Blockade forbids population of  $|2, 0\rangle$ . The population of the  $|b\rangle$  state will then be either 0, 1, or 2 atoms.

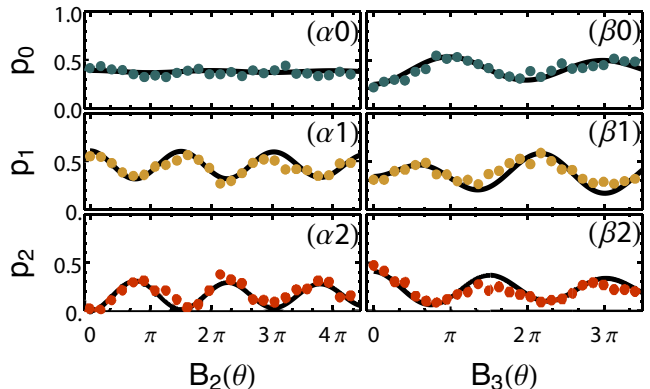


FIG. 4. (Color online) ( $\alpha$ ) Evolution of  $N_b=0, 1$  and  $2$  atom populations using the  $A_1B_1A_2B_2(\theta)$  protocol. ( $\beta$ ) Output of the  $\mathcal{N} = 2$  Fock state production as a function of  $B_3$  area.

Figure 4( $\alpha$ ) shows the probabilities for observing 0, 1, or 2 atoms in state  $|b\rangle$  after the  $A_1B_1A_2B_2(\theta)$  sequence. As expected, the probability of observing two atoms, Fig. 4( $\alpha 2$ ), begins at 0 and oscillates at  $\sqrt{2}\Omega_1$ . Note that the decay time of the two atom collective oscillation is set by the same decoherence processes as would be observed in single atom-atom Rabi oscillations, and there is no additional dephasing from atom number fluctuations because exactly two atoms participate in the oscillation. The  $N_b = 0$  signal, Fig. 4( $\alpha 0$ ), potentially has contributions from the single atoms states  $|0, 1\rangle$  and  $|1, 0\rangle$ , but these oscillations are out of phase and cancel

if the populations of those states are equal, as is nearly the case for this data.

The  $N_b = 1$  signal, Fig. 4( $\alpha$ 1), potentially has contributions from Rabi oscillations of the states  $(|1, 0\rangle, |0, 1\rangle, |1, 1\rangle)$  at frequencies  $(1, 1, \sqrt{2})\Omega_1$ . Again, the first two are cancelled if their populations are equal, leaving only the collective 2-atom signal.

The probability of producing the Fock state  $|0, 2\rangle$  is 32% for this data, for which the FORT drop time was extended to  $6.34 \mu\text{s}$  to see 3 full collective Rabi oscillations. As a result, additional high velocity atoms are not recaptured when the FORT is restored, reducing the signal size. For  $2 \mu\text{s}$  FORT drops, we have observed up to  $48 \pm 2\%$   $N_b = 2$ . For example, the state produced at the beginning of Fig. 4( $\beta$ ) has  $Q = -0.50 \pm 0.05$ .

The full  $F = 2$  Fock sequence can be further probed by restoring the FORT for 0.5 ms, enough to eject any Rydberg population from  $|1, 0\rangle$  and  $|1, 1\rangle$ , effectively leaving only ground-state populations in the states  $|0, 0\rangle, |0, 1\rangle$ , and  $|0, 2\rangle$ . This removes the cancellation between the  $|0, 1\rangle$  and  $|1, 0\rangle$  signals observed in Fig. 4( $\alpha$ ). Now, as shown in Fig. 4( $\beta$ ), oscillations at  $\Omega_1$  are observed in the  $N_b = 0$  data, and the  $N_b = 1$  data have both  $\Omega_1$  and  $\sqrt{2}\Omega_1$  signals superposed. The fits to the oscillations have only the 3 initial state populations as adjustable parameters, and assume no atom number fluctuations.

Both the  $N_b = 1$  and  $N_b = 2$  Fock state populations are consistent with a single collective  $AB$  sequence success probability of  $0.65 - 0.70$ . In Fig. 5 we show the  $\mathcal{N} = 1$  Fock state population as a function of  $\bar{N}$ . We also show the results of a quantum Monte Carlo model of a collective  $A_1B_1$  pulse sequence. The model considers the known significant sources of experimental imperfections, which include Doppler shifts, the distribution of AC-Stark shifts and Rabi frequencies from the Gaussian intensity distributions, spontaneous emission from the intermediate  $5p$  state (spontaneous emission from the Rydberg states is negligible on  $5 \mu\text{s}$  timescales), and  $1 \mu\text{m}$  misalignments of the excitation lasers. For a single atom, the model reproduces our observed  $AB$  success probability of 85%. For multiple atoms, the model allows both single and double Rydberg excitations. The double excitations during the A portion of the sequence primarily consist of atom pairs at extreme ends of the cloud. Those double excitations still experience some Rydberg-Rydberg interactions, and therefore are off-resonant for the B deexcitation portion of the sequence, thereby suppressing the number of occurrences of  $N_b = 2$ . The lines in Fig. 5 show, from highest to lowest, the predicted fidelity assuming perfect Rabi flopping and infinite blockade; experimental imperfections with infinite blockade; and finally including both experimental imperfections and finite blockade. The black dashed curve corresponds to the fit parameter  $\epsilon = 1$  in Eq. 1.

Using this information, the predicted Fock state sequence fidelity should reach 80% by  $\bar{N} = 7$ . This is

15% higher than we observe in the experiment, and gets slightly worse with increasing  $\bar{N}$ . The source of the additional inefficiency is unknown to us, but we note that our densities,  $5N \times 10^{10} \text{ cm}^{-3}$ , approach peak densities where laser cooling limits are observed due to multiple scattering. We note that recent results on using Rydberg blockade for single-photon sources [8] found a  $67 \pm 10\%$  preparation efficiency of the singly-excited many-body state at similar atom densities.

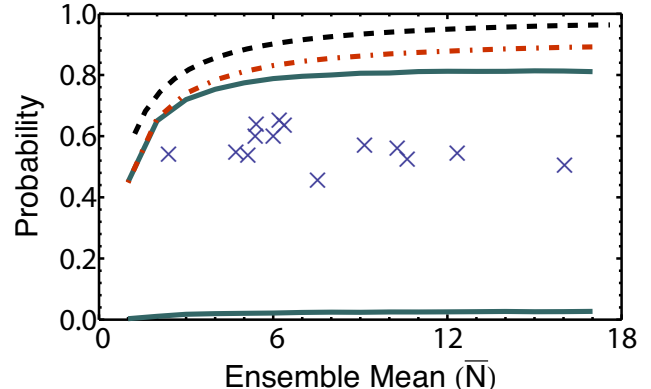


FIG. 5. (Color online)  $\mathcal{N} = 1$  Fock state production fidelity as a function of mean ensemble number, and quantum Monte Carlo simulations. The black dashed line assumes ideal blockade and perfect excitation conditions. The red dot-dashed line adds in realistic experimental imperfections, and the green solid line includes finite blockade strength. The solid green line at the bottom shows the predicted 2-atom production.

The Q-parameter for deterministic  $\mathcal{N} = 1$  schemes studied to date give: collisional blockade using light assisted collisions,  $Q = -0.5$  [19, 20]; this work,  $Q = -0.65$ , repulsive light-assisted collisions,  $Q = -0.91$  [21]; and Mott-insulator samples,  $Q = -0.95$  [22]. For  $\mathcal{N} = 2$  with  $Q = -0.5$ , other methods to date require cooling to quantum degeneracy: the  $\mathcal{N} = 2$  shell of a Mott insulator [22], or controlled spilling from a degenerate Fermi gas [23]. Both achieve  $Q < -0.9$ .

Our studies of Rydberg-blockade-mediated collective Rabi flopping show that the collective Rabi frequencies very closely follow the predicted  $\Omega_N = \sqrt{N}\Omega_1$  dependence. This, plus our observation of the lack of two atom production in an  $A_1B_1$  sequence, strongly imply that the blockade phenomenon is highly effective at rejecting double Rydberg excitations. We used the collective flopping to produce a strongly sub-Poissonian atom distribution with  $Q = -0.65$  in a single trap site. Extending the protocol to a 2 atom Fock state, we get  $Q = -0.5$  and observe 3 cycles of  $N = 2$  collective Rabi flopping with no additional dephasing. Future plans include producing blockaded samples with higher numbers of atoms at lower densities, where possible density dependent mechanisms should be lessened.

Important contributions at early stages of this work

were made by Erich Urban, Thomas Henage, and Larry Isenhower, and we acknowledge helpful discussions with Klaus Mølmer. This work was funded by NSF grant #PHY-1104531 and the AFOSR Quantum Memories MURI.

---

\* mebert@wisc.edu

- [1] M. D. Lukin, M. Fleischhauer, R. Cote, L. M. Duan, D. Jaksch, J. I. Cirac, and P. Zoller, *Phys. Rev. Lett.*, **87**, 037901 (2001).
- [2] M. Saffman, T. G. Walker, and K. Mølmer, *Rev. Mod. Phys.*, **82**, 2313 (2010).
- [3] E. Urban, T. A. Johnson, T. Henage, L. Isenhower, D. D. Yavuz, T. G. Walker, and M. Saffman, *Nature Phys.*, **5**, 110 (2009).
- [4] A. Gaëtan, Y. Miroshnychenko, T. Wilk, A. Chotia, M. Viteau, D. Comparat, P. Pillet, A. Browaeys, and P. Grangier, *Nature Phys.*, **5**, 115 (2009).
- [5] T. Wilk, A. Gaëtan, C. Evellin, J. Wolters, Y. Miroshnychenko, P. Grangier, and A. Browaeys, *Phys. Rev. Lett.*, **104**, 010502 (2010).
- [6] L. Isenhower, E. Urban, X. L. Zhang, A. T. Gill, T. Henage, T. A. Johnson, T. G. Walker, and M. Saffman, *Phys. Rev. Lett.*, **104**, 010503 (2010).
- [7] X. L. Zhang, L. Isenhower, A. T. Gill, T. G. Walker, and M. Saffman, *Phys. Rev. A*, **82**, 030306(R) (2010).
- [8] Y. O. Dudin, L. Li, F. Bariani, and A. Kuzmich, *Nature Physics*, **8**, 790 (2012).
- [9] T. Peyronel, O. Firstenberg, Q.-Y. Liang, S. Hofferberth, A. V. Gorshkov, T. Pohl, M. D. Lukin, and V. Vuletic, *Nature*, **488**, 57 (2012).
- [10] Y. O. Dudin and A. Kuzmich, *Science*, **336**, 887 (2012).
- [11] D. Maxwell, D. J. Szwer, D. Paredes-Barato, H. Busche, J. D. Pritchard, A. Gauguier, K. J. Weatherill, M. P. A. Jones, and C. S. Adams, *Phys. Rev. Lett.*, **110**, 103001 (2013).
- [12] J. Honer, R. Löw, H. Weimer, T. Pfau, and H. P. Büchler, *Phys. Rev. Lett.*, **107**, 093601 (2011).
- [13] L. Li, Y. O. Dudin, and A. Kuzmich, *Nature*, **498**, 466 (2013).
- [14] I. I. Beterov, M. Saffman, E. A. Yakshina, V. P. Zhukov, D. B. Tretyakov, V. M. Entin, I. I. Ryabtsev, C. W. Mansell, C. MacCormick, S. Bergamini, and M. P. Fedoruk, *Phys. Rev. A*, **88**, 010303 (R) (2013).
- [15] M. Saffman and T. G. Walker, *Phys. Rev. A*, **66**, 065403 (2002).
- [16] M. Saffman and T. G. Walker, *Phys. Rev. A*, **72**, 042302 (2005).
- [17] T. G. Walker and M. Saffman, *Phys. Rev. A*, **77**, 032723 (2008).
- [18] The signal calibrations are described in the Supplemental Material at <http://digital.library.wisc.edu/1793/66913>.
- [19] M. T. DePue, C. McCormick, S. L. Winoto, S. Oliver, and D. S. Weiss, *Phys. Rev. Lett.*, **82**, 2262 (1999).
- [20] N. Schlosser, G. Reymond, and P. Grangier, *Phys. Rev. Lett.*, **89**, 023005 (2002).
- [21] A. V. Carpentier, Y. H. Fung, P. Sompert, A. J. Hilliard, T. G. Walker, and M. F. Andersen, *Laser Phys. Lett.*, **10**, 125501 (2013).
- [22] W. S. Bakr, A. Peng, M. E. Tai, R. Ma, J. Simon, J. I. Gillen, S. Fölling, L. Pollet, and M. Greiner, *Science*, **329**, 547 (2010).
- [23] F. Serwane, G. Zürn, T. Lompe, T. B. Ottenstein, A. N. Wenz, and S. Jochim, *Science*, **332**, 336 (2011).